A selective, cell-permeable fluorescent probe for Al^{3+} in living cells†

Lina Wang, Wenwu Qin, Xiaoliang Tang, Wei Dou, Weisheng Liu,* Qingfeng Teng and Xiaojun Yao

Received 13th May 2010, Accepted 8th June 2010
First published as an Advance Article on the web 8th July 2010
DOI: 10.1039/c0ob00123f

The synthesis and evaluation of a novel Schiff-base fluorescent probe **L** for detection of Al^{3+} are described. The structure of **L** was determined by X-ray and other spectroscopic data. The fluorescent spectra changes and microscopy images show that indicator **L** is highly selective for Al^{3+} not only in abiotic systems but also in living cells. Other metal ions failed to respond. The new probe could be used as an efficient tool for Al^{3+} monitoring in the environment and biological systems.

Introduction

Compounds of aluminium are widely dispersed and used in the environment around us in modern society: in water treatment, in food additives, in medicines, and of course, as the production of light alloys, *etc.* It is well-known that aluminium is not an essential element for biological life and its toxicity is a concern for human health. Recent advances have shed light on the biological roles of aluminium, particularly on its functions related to neurobiology. Disorders of aluminium homeostasis are implicated in a number of diseases, such as Parkinson's disease.[1] High contents of aluminium in the body can do harm to the brain and kidneys.[2,3] Aluminium can also damage eco-environmental and biological samples, and it builds-up due to the wide use of aluminium products and water purification by aluminium salts. Therefore, methods to detect chelatable aluminium (Al^{3+}) in biological studies have attracted much attention recently. There is a great need for the design and synthesis of Al^{3+} chemosensors which have high sensitivity and selectivity for detecting and monitoring. Fluorescent probes for real-time sensing of biologically important ions and fluorescence imaging have become indispensable tools in numerous fields of modern medicine and science.[4] The design, synthesis, and spectroscopic characterization of novel fluorescent probes for metal ion analysis remains an active research field. Fluorescence offers significant advantages over other methods for metal ion measurement inside living cells because of its generally non-destructive character, high sensitivity, instantaneous response, and the wide range of indicator dyes available.[5]

The detection of Al^{3+} has always been problematic due to the lack of spectroscopic characteristics and poor coordination ability compared to transition metals.[6] Few Al^{3+} fluorescence probes have been reported, and the majority of the reported Al^{3+} sensors have poor water solubility.[7] In the last decades, particular attention has been paid to the synthesis and study of metal complexes of Schiff bases.[8] This is due to several reasons: some of the Schiff base metal complexes have antitumor properties,[9] antioxidative activities,[10] and attractive electronic and photophysical properties.[11] In addition, Schiff base derivatives incorporating a fluorescent moiety are appealing tools for optical sensing of metal ions. In our report, we synthesized one Schiff-base chemosensor 2-hydroxybenzene-1-carbohydrazide-1-(benzo[1,3]-oxazino[2,3-a] phthalazin-4-one) (compound **L**), which was designed to chelate with metal ions *via* its carbonyl O and imino N atoms. **L** is a very promising Al^{3+}-specific fluorescent host in HEPES buffer solution (water–ethanol = 99/1, v/v, pH 7.4) and other solvents upon intramolecular charge transfer (ICT) and chelation-enhanced fluorescence (CHEF). The ICT mechanism and CHEF mechanism are attractive design principles for developing luminescent chemical devices. The reduction of ICT results in enhanced fluorescence emission, and CHEF is caused by using structurally simple conjugation between ligand and cation. In sensor **L**, taking advantage of the lone electron pairs on N and O, the ligand can effectively coordinate with the appropriate ion. Upon complexation with a certain metal ion, a large CHEF effect is observed because of the rigid framework: the reaction of a metal ion with a chelating agent induces rigidity in the resulting molecule and tends to produce fluorescence. Simultaneously, upon the capture of a metal ion, the excited ICT of the ligand would become weak by reduction of either the electron-accepting ability of the oxygen-containing group or the electron-donating ability of the amine unit.

Result and discussion

As mentioned above, Schiff-base derivatives have many good antibacterial activity and spectroscopic properties. As part of a project on the synthesis and study of Schiff-bases for fluorescence probes, we recently designed a ligand **L**. It was facilely synthesized from the reaction of salicylhydrazide with *ortho*-phthalaldehyde (Scheme 1). The molecular structure and its purity were confirmed

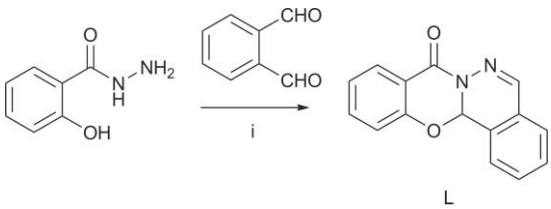

Scheme 1 Synthesis of the fluorescent indicator **L**. Reagents and conditions: (i) ethanol, reflux, 8 h, 69%.

Key Laboratory of Nonferrous Metal Chemistry and Resources Utilization of Gansu Province and State Key Laboratory of Applied Organic Chemistry, College of Chemistry and Chemical Engineering, Lanzhou University, Lanzhou 730000, P. R. China. E-mail: liuws@lzu.edu.cn; Fax: +86-0931-8912582; Tel: +86-0931-8915151

† Electronic supplementary information (ESI) available: IR; ^{1}H-NMR; ^{13}C-NMR; ESI-MS. CCDC reference number 746902. For ESI and crystallographic data in CIF or other electronic format see DOI: 10.1039/c0ob00123f

by NMR and MS (ESI),† and this was unequivocally corroborated on the basis of the single-crystal X-ray analysis (Fig. 1).

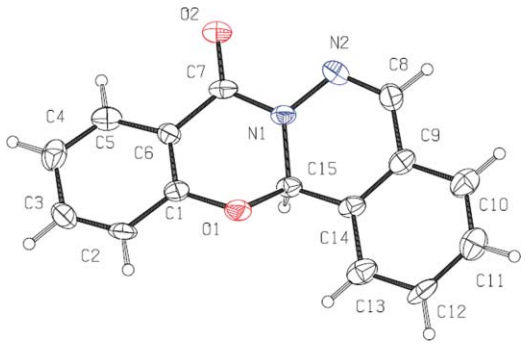

Fig. 1 ORTEP diagram of the compound **L** (30% probability level for the thermal ellipsoids).

Fluorescence sensors based on electron donor/acceptors are usually disturbed by protons in the detection of metal ions, so it is necessary to investigate the effects of pH on the sensor **L** and find optimal sensing conditions. Fluorescence pH titrations of the sensor were carried out in aqueous ethanol (99/, v/v) solution (Fig. 2) to identify the conditions under which the metal sensing ability of **L** could be probed. The optimal pH (7.4) is near physiological pH, which indicates that **L** could be applied as an Al^{3+} sensor in biological organisms or in medical research. There is no change in the fluorescence spectrum of **L** observed after the addition of Al^{3+} at a pH below 3.3, which can be reasonably related to the combination of protons with N atoms in –C=N– groups, which inhibits the coordination of Al^{3+} with **L**. On the other hand, the fluorescence of **L** has no response to Al^{3+} at high pH values, which could be due to competition of OH^- ions with probe **L** for the sensing of Al^{3+}.

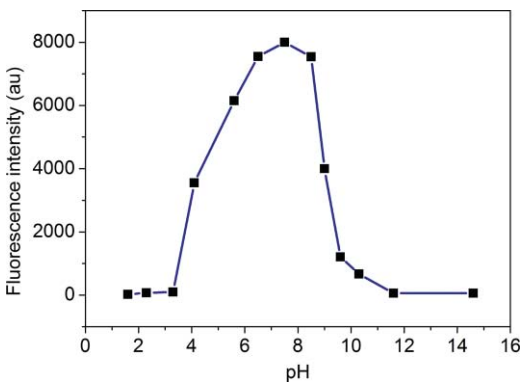

Fig. 2 Effect of pH on the fluorescence intensity of **L** (0.1 mM) at 406 nm in the presence of 0.5 equiv. of Al^{3+} in ethanol–H_2O (1/99, v/v) solution. Excitation was provided at 330 nm.

The fluorescence spectra properties of **L** (40 μM) were investigated in 99 : 1 HEPES-buffered aqueous ethanol. The fluorescence emission band of **L** at 435 nm is very weak. The addition of Al^{3+} ion afforded a significant enhancement in fluorescence intensity of **L**, with a blue shift from 435 nm to 406 nm, it increased from 29 to 2963 as the concentration of Al^{3+} reached 36 μM (Fig. 3). The reasons for the large changes in emission spectra are as follows: in the absence of Al^{3+} ions, the extent of ICT in the ligand **L** was efficient and the fluorescence was effectively quenched. The coordination of **L** with Al^{3+} ion induced the reduction of the ICT effect (effectively unquenching) in the ligand, which caused the significant enhancement in fluorescence intensity accompanied by a blue shift. In addition, the enhancement of the fluorescence intensity was due to the formation of a **L**–Al^{3+} complex, which resulted in the selective CHEF effect. No change in the fluorescence spectra could be found after adding the same concentration of other ions, such as Li^+, Na^+, Mg^{2+}, K^+, Ca^{2+}, Mn^{2+}, Fe^{3+}, Co^{2+}, Ni^{2+}, Cu^{2+}, Zn^{2+}, Ag^+, Cd^{2+}, Hg^{2+} and Pb^{2+} to the aqueous solution of **L**.

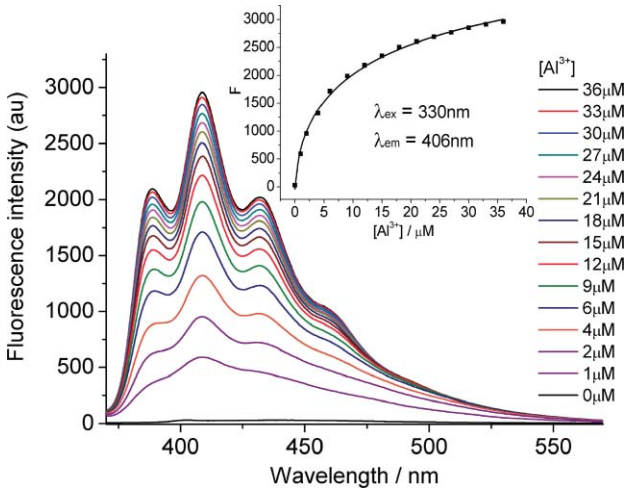

Fig. 3 Fluorescence emission spectra of **L** (40 μM) with addition of various concentrations of $Al(ClO_4)_3$ (0–36 μM) in HEPES-buffered solution (ethanol–H_2O = 1/99, v/v, pH 7.4) and λ_{ex} = 330 nm. Each spectrum was acquired 5 min after Al^{3+} addition. Inset: the best fits of eqn (1) using the direct fluorometric titration method to the fluorometric titration data of **L** obtained from the emission spectra ($n = 0.5$).

The fluorescence titration experiments were performed by mixing various amounts of metal ions with a constant concentration of **L** in HEPES-buffered solution (water–ethanol = 99 : 1, v/v, pH 7.4). The fluorescence emission changes of **L** in the presence of various concentrations of Al^{3+} are shown in Fig. 3. The fluorescence intensity enhanced gradually with the increase of Al^{3+}. The ground-state dissociation constant K_d of the complex between **L** and Al^{3+} was determined by direct fluorimetric titration as a function of the cation concentration [X] (X = Al^{3+}) using the fluorescence emission spectra (Fig. 3). Non-linear fitting of eqn (1)[12] to the steady-state fluorescence data F recorded as a function of [X] yields a values of K_d of 6.1 μM. F_{min} and F_{max} represent the fluorescence signals at maximal and minimal [Al^{3+}], n represents the number of aluminium ions bound per probe. Because the fits of eqn (1) to the fluorescence data F with n, K_d, F_{min}, and F_{max} as freely adjustable parameters always gave values of n close to 0.5, n was kept fixed at 0.5 in the final curve fittings. The value of n indicated a 2 : 1 stoichiometry for the **L**–Al^{3+} complex. This binding mode was also supported by the data of Job's plots (Fig. 4).[13]

$$F = \frac{F_{max}[X]^{n} + F_{min}K_d}{K_d + [X]^{n}} \quad (1)$$

The detection limit was calculated based on the fluorescence titration. The emission intensity of **L** without Al^{3+} was measured

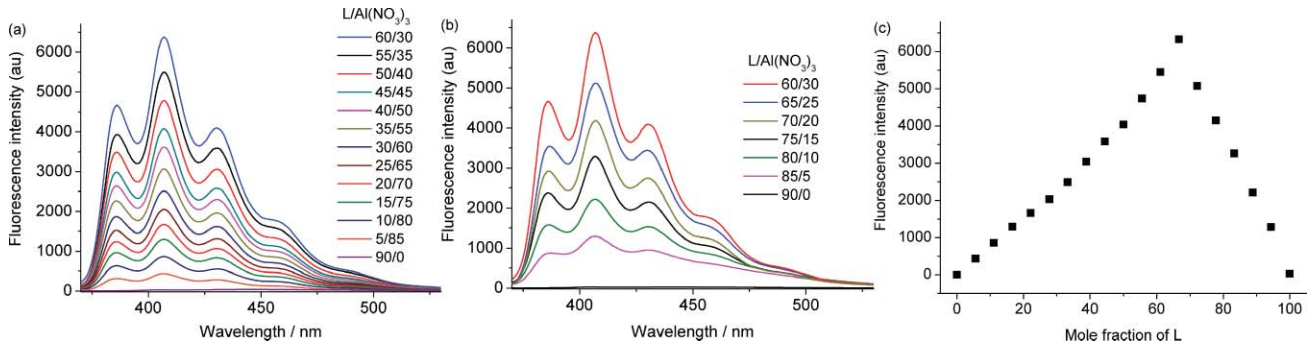

Fig. 4 (a, b) Fluorescence emission spectra of various concentrations of **L** with addition of varying amounts of $Al(ClO_4)_3$ in ethanol with λ_{ex} = 330 nm. Each spectrum was acquired 5 min after mixing **L** and Al^{3+} ions. (c) Plots according to the method for continuous variations, indicating the 2 : 1 stoichiometry of the **L**–Al^{3+} complex. The total concentration of **L** and Al^{3+} ions is 90 μM.

10 times and the standard deviation of blank measurements was determined. A good linear relationship between the fluorescence intensity and the Al^{3+} concentration could be obtained in the 0–2.25 μM concentration range ($R^2 = 0.9878$; Fig. 5). The detection limit was then calculated with the equation: detection limit = $3\sigma_{bi}/m$, where σ_{bi} is the standard deviation of blank measurements, m is the slope between intensity *versus* sample concentration. The detection limit was measured to be 8.8×10^{-9} M. According to China EPA standard, Al^{3+} concentrations lower than 0.05 mg L^{-1} (1.85 μM) are acceptable in drinking water. This means that our proposed fluorescent method based on probe molecule **L** is sensitive enough to monitor the water quality of drinking water.

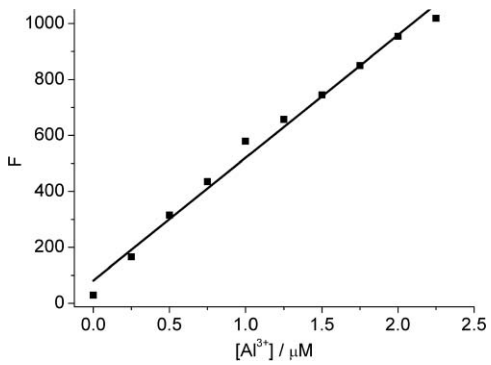

Fig. 5 Fluorescence intensity at 406 nm for **L** (40 μM) in HEPES-buffered solution (ethanol–H_2O = 1/99, v/v, pH 7.4) as a function of the concentration of Al^{3+}. The excitation wavelength for the complex was 330 nm.

Achieving high selectivity for the analyte of interest over a complex background of potentially competing species is a challenging task in sensor development. Fig. 6 shows the fluorescence response of **L** to Al^{3+} in the presence of alkali, alkaline earth, and transition metal ions in HEPES-buffered solution (water–ethanol = 99/1, v/v, pH 7.4). A background of most selected coexistent metal ions does not interfere with the sensing of **L** for Al^{3+}. The addition of Zn^{2+} to the solution containing **L** and Al^{3+} can induce an increase of the fluorescence intensity, but the existence of Al^{3+} ion in solution can be detected by fluorescent probe **L** without interference.

We also investigated the possibility of using fluorescent chemosensor **L** for the detection of Al^{3+} in other solvents, such

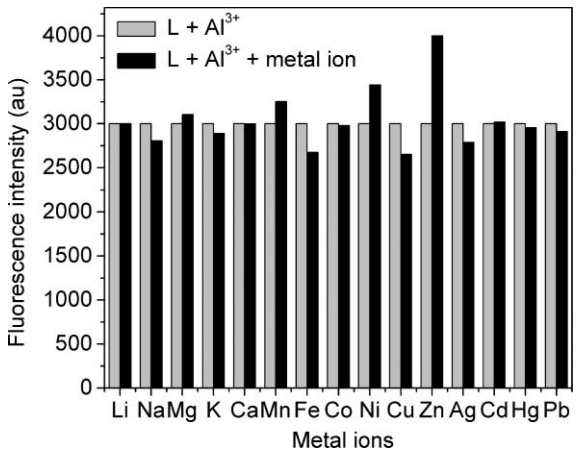

Fig. 6 Metal-ion selectivity of **L** (40 μM) in HEPES buffer solution (water–ethanol = 99/1, v/v, pH 7.4) with excitation at 330 nm. The gray bars represent the fluorescence emission of solution of **L** and 0.5 equiv. of Al^{3+}. The black bars show the fluorescence change that occurs upon addition of 0.5 equiv. of the corresponding cation to the solution containing **L** and 0.5 equiv. of Al^{3+}.

as methanol, ethanol, acetone, *N*,*N*-dimethylformamide (DMF), dimethyl sulfoxide (DMSO), acetonitrile, toluene, chloroform and dichloromethane. The fluorescence intensity was largely enhanced with the addition of Al^{3+} in some other solvents of **L**, such as methanol, ethanol, DMF, and DMSO (Fig. 7), and there was a tiny increase in acetone and acetonitrile. Changes of the fluorescence intensity of **L** in the presence of Al^{3+} in toluene, chloroform and dichloromethane could be considered negligible. It may be caused by the non-protic nature or poor coordination ability of solvents. As is well known, water, methanol, ethanol, DMF and DMSO all contain an oxygen atom which is easily coordinated, but there is not such an easily-coordinated atom in other solvents. So we speculate that solvent molecules take part in the coordination.

Fig. 8 illustrates the change of UV-vis spectra of probe **L** in HEPES-buffered solution (H_2O–ethanol = 99/1, v/v, pH 7.4) in the presence of Al^{3+}. The absorption spectrum of **L** in ion-free solution presents two important transitions with intense absorption bands at 298 and 232 nm. The band at 298 nm is attributed to the azomethine C=N bond and the band at 232 nm is assigned to carbonyl C=O. The two absorption bands both changed as the concentration of Al^{3+} increased, accompanying

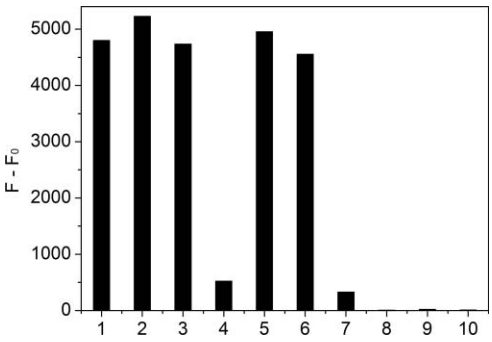

Fig. 7 Fluorescence intensity changes of **L** at 406 nm (50 μM) in the absence (F_0) and presence (F) of 0.5 equiv. of Al^{3+} in different solvents. 1-Ethanol–H_2O (1 : 99, v/v); 2-methanol; 3-ethanol; 4-acetone; 5-DMF; 6-DMSO; 7-acetonitrile; 8-toluene; 9-chloroform; 10-dichloromethane. $\lambda_{ex} = 330$ nm.

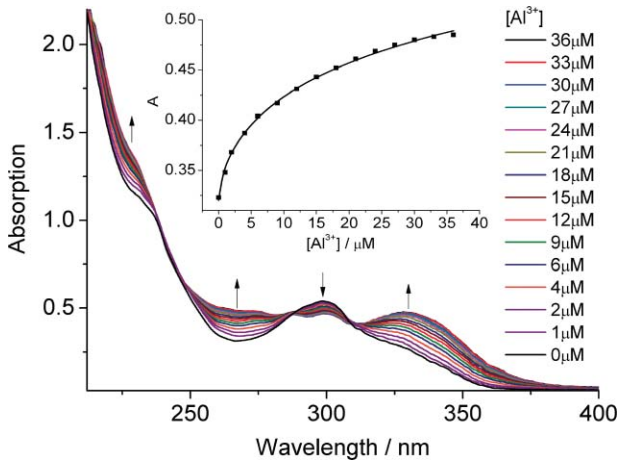

Fig. 8 Absorption spectra of **L** (40 μM) in HEPES buffer solution (water–ethanol = 99/1, v/v, pH 7.4) with addition of various concentrations of $Al(ClO_4)_3$ (0–36 μM). Inset: the best fits of eqn (1) using the direct UV-spectra titration method to the UV-spectra titration data of **L** obtained from the absorption spectra at 330 nm ($n = 0.5$).

three isosbestic points at 309, 288 and 243 nm. There are four changes upon the addition of Al^{3+} ions. Firstly, a new peak emerges at 330 nm, which indicated the new complex **L**–Al^{3+} formed. Secondly, the absorption peak at 298 nm declined, which suggests that the C=O takes part in the coordination. Thirdly, the absorption band centered around 267 nm increased. Finally, the band at 232 nm increased, which may be caused by the nitrogen of azomethine being involved in the formation of the complex **L**–Al^{3+}. The change of the spectra indicates that the **L**–Al^{3+} complex may be formed during the addition of Al^{3+}. The intensity of the new peak changes regularly with the continuous increase of Al^{3+} concentration. The nonlinear fitting of the titration curve assumed a 2 : 1 stoichiometry for the **L**–Al^{3+} complex with an association constant K_a value of 9.0 μM (Fig. 8, inset).

Comparing the IR spectra of the **L**–Al^{3+} complex with that of the "free" ligand, we can see two differences: firstly, the stretch vibration of the carbonyl group (C=O) at 1694 cm^{-1} with a weak and broad band changes to a strong and sharp absorption band at 1614 cm^{-1}; secondly, the stretching vibration of the aromatic aldimine (C=N) at 1643 cm^{-1} splits into two strong and sharp absorption bands at 1541 and 1484 cm^{-1} (ESI).† These differences suggest that the carbonyl group and aromatic aldimine take part in the coordination with Al^{3+}. The spectra properties of **L** in other solvents indicate that solvent molecules take part in coordination. It is well-known that most Al complexes are hexacoordinated.[14] Therefore, according to the above data and some crystal structures of Schiff-base compounds, we propose the reaction mechanism shown in Fig. 9. In Fig. 9, a single nuclear aluminium complex is formed. Solvent molecules offer two coordination sites. More direct evidence was obtained by the ESI mass spectra of **L**–Al^{3+} (ESI).† The peaks at $m/z = 617.3$ (calcd = 617.2) and $m/z = 589.1$ (calcd = 589.2) corresponding to $AlL_2(CH_3CH_2O)_2$ and $AlL_2(CH_3O)_2$ were observed, respectively. Coordination of **L** with Al^{3+} forms a rigid conjugation system, two ligands and the Al^{3+} ion in the system in a plane, which causes a large CHEF effect and reduces the ICT effect in the ligand. As a result, the emission peak in the fluorescence spectrum shows a significant enhancement with a blue shift. However, other metal ions failed to form such a rigid framework. We presume the unique selectivity of Al^{3+} can be interpreted in terms of smaller radii (0.5 Å) and larger charge density ($\rho = 4.81$) of the Al^{3+} ion. The smaller radii of Al^{3+} ion accord with suitable coordination geometry of the chelating receptor **L**, moreover, the larger charge density affords strong coordination ability between **L** and Al^{3+}.

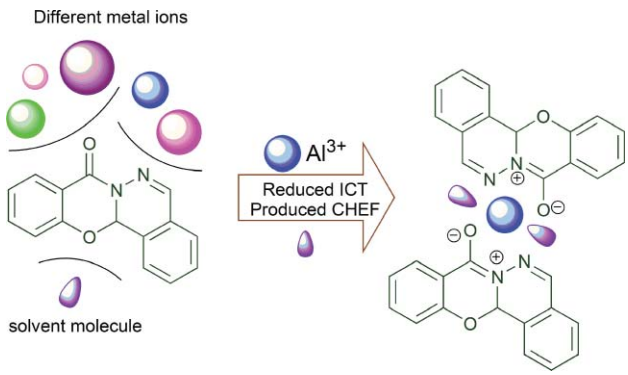

Fig. 9 Proposed mechanism for the fluorescence enhancement of **L** upon the addition of Al^{3+}.

In order to confirm the structure of the **L**–Al^{3+} complex, density functional theory (DFT) calculations were performed using the G98 program package. The B3LYP exchange functional was used in this calculation, 6-31G(d) basis sets were used, except for Al^{3+}, where the LANL2DZ effective core potential (ECP) was employed. The optimized configuration is shown in Fig. 10, which shows the coordination number equal to 6, the two organic ligands nearly in a plane and the water molecules in a vertical line. The Al–N bond length is 2.03 Å, and the Al–O bond lengths are 1.86 Å (Al–O_L) and 2.04 Å (Al–O_{water}), respectively.

Subsequent experiments probed the ability of **L** to track Al^{3+} levels in living cells using fluorescence microscopy. To determine the cell permeability of **L**, human leukemia K562 cells were incubated with **L**. HL K562 cells incubated with 50 μM **L** for up to 30 min at 37 °C show negligible intracellular fluorescence. In contrast, **L**-stained cells exposed to 25 μM Al^{3+} for 30 min at 37 °C display enhanced cytosolic fluorescence (Fig. 11). Experiments

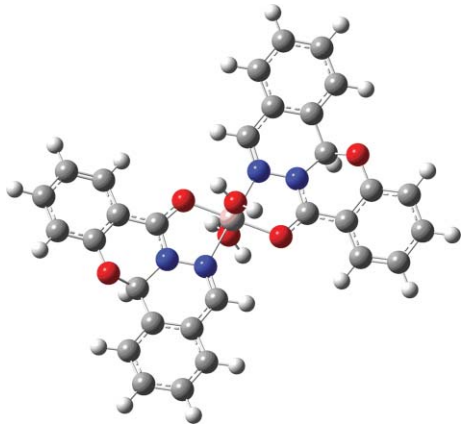

Fig. 10 Calculated energy-minimized structure of **L** with Al^{3+}.

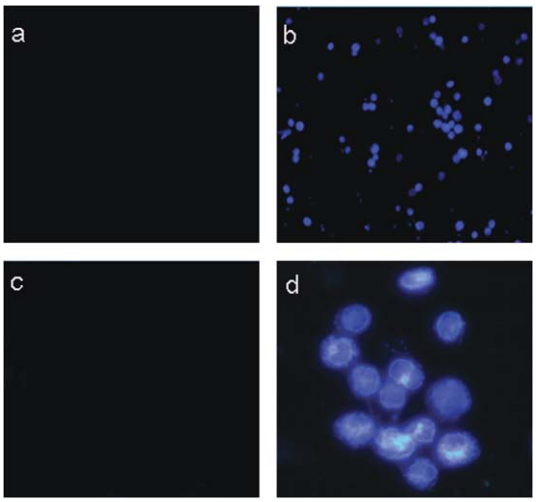

Fig. 11 Fluorescence microscope images of human leukemia K562 cells: human leukemia K562 cells loaded with probe **L** (50 μM) for 30 min under 10× objective lens (a) and 40× objective lens (c). Fluorescence image of **L**-stained human leukemia K562 cells exposed to 25 μM Al^{3+} for 30 min under 10× objective lens (b) and 40× objective lens (d). Incubation was performed at 37 °C.

without ligand **L** or Al^{3+} give no fluorescence over background levels. Taken together, it clearly demonstrated that the probe is membrane-permeable, and the fluorescence change in the human leukemia K562 cells was really due to the synchronous presence of **L** and Al^{3+}. The result confirmed that the probe **L** can be used to image intracellular Al^{3+} in living cells. It should therefore be potentially useful for the study of the toxicity or bioactivity of Al^{3+} in living cells.

Conclusion

In summary, we have designed and prepared one Schiff-base fluorescent chemosensor **L** and investigated its chemosensing properties. The sensor **L**, containing lone electron pairs on N and O, exhibits high selectivity for Al^{3+} ions not only in abiotic systems but also in living cells, presumably due to a combinational effect of ICT and CHEF during the chelation of **L** toward the Al^{3+} ion in a 2 : 1 complex mode. In addition, the formation of the **L**–Al^{3+} complex relies on a specific conformation of the Schiff-base ligand, suitable radius and larger charge density of metal ion, sensitive fluorophore and suitable protic solvent. The strategy will help us design more chemosensors, which have ideal chemical and spectroscopic properties that can be applied in environmental monitoring and medical research.

Experimental section

Spectroscopic measurements

^1H and ^{13}C NMR spectra were taken on a Varian Mercury-300 spectrometer with TMS as an internal standard and DMSO-d_6 as solvent. Chemical shift multiplicities are reported as s = singlet, d = doublet, t = triplet, q = quartet and m = multiplet. HRMS was determined on a Bruker Daltonics APEXII 47e FT-ICR mass spectrometer. IR spectra were recorded on a Nicolet FT-170SX instrument using KBr discs in the 400–4000 cm^{-1} region. Melting points were determined on a Kofler apparatus. Absorption spectra were determined on a Varian UV-Cary100 spectrophotometer using quartz cells of 1.0 cm path length. Fluorescence spectra measurements were performed on a Hitachi F-4500 spectrofluorimeter and a Shimadzu RF-540 spectrofluorophotometer equipped with quartz cuvettes of 1 cm path length with a xenon lamp as the excitation source. An excitation and emission slit of 5.0 nm were used for the measurements in the solid state. All pH measurements were made with a pH-10C digital pH meter. All spectra were recorded at room temperature except for fluorescence microscope images. The fluorescence microscope experiment was carried out with a Olympus AX-80.

All the materials for synthesis were purchased from commercial suppliers and used without further purification. Deionized water was used as solvent. All of the solvents used were of analytical reagent grade. The solutions of metal ions were prepared from their perchloride salts, except for KNO_3. HEPES-buffered solution (pH = 7.4) was prepared in double-distilled water.

Crystal structure determination‡

Single crystals of compound **L** suitable for X-ray diffractometry were obtained by dissolving powder of the pure compound in EtOH and slow evaporation of the solution free from vibrations. These were mounted in inert oil and transferred to the cold gas stream of the diffractometer. Single-crystal X-ray diffraction measurements were carried out on a Bruker SMART 1000 CCD diffractometer operating at 50 KV and 30 mA using Mo-Kα radiation ($\lambda = 0.71073$ Å). The selected crystal was mounted inside a Lindemann glass capillary for data collection using the SMART and SAINT software. An empirical absorption correction was applied using the SADABS program. All the structures were solved by direct methods and refined by full-matrix least-squares on F^2 using the SHELXTL-97 program package.[15] All non-hydrogen atoms were subjected to aniostropic refinement, and all hydrogen atoms were added in idealized positions and refined isotropically. A multipurpose crystallographic tool, PLATON, was used for molecular graphics.[16] Relevant crystallographic information is summarized in Table 1. Full crystallographic data,

‡ Crystallographic data in CIF format for compound **L** is given in the electronic supplementary information (ESI).

Table 1 Crystal data

Compound	**L**
Chemical formula	$C_{15}H_{10}N_2O_2$
Formula Mass	250.25
Crystal system	Monoclinic
a/Å	12.022(5)
b/Å	11.403(5)
c/Å	17.406(10)
α (°)	90.00
β (°)	95.445(11)
γ (°)	90.00
Unit cell volume/Å^3	2375(2)
T/K	293(2)
Space group	*Cc*
No. of formula units per unit cell, *Z*	8
No. of reflections measured	5422
No. of independent reflections	2585
R_{int}	0.0433
Final R_1 values ($I > 2\sigma(I)$)	0.0703
Final w$R(F^2)$ values ($I > 2\sigma(I)$)	0.1604
Final R_1 values (all data)	0.1002
Final w$R(F^2)$ values (all data)	0.1826

excluding structure factors, have been deposited at the Cambridge Crystallographic Data Centre. CCDC reference number 746902.†

2-Hydroxybenzene-1-carbohydrazide-1-(benzo[1,3]-oxazino[2,3-a]phthalazin-4-one) (L)

Salicylhydrazide (1.520 g, 10.0 mmol) was dissolved in a 100 mL three-necked flask with hot ethanol (25 mL), then refluxed until the salicylhydrazide was dissolved completely, Next a solution (15 mL) of *ortho*-phthalaldehyde (1.342 g, 10.0 mmol) was added and the reaction mixture was refluxed for 8.0 h. The solvent was evaporated and a thick liquid appeared. Subsequently, 50 mL distilled water was dumped into the thick liquid to give the product as brown particles, **L** (1.720 g, 6.88 mmol) was gained in 68.8% yield. The desired single crystals of compound **L** were obtained by dissolving powder of the product in EtOH and slow evaporation of the solution over 36 h free from vibrations. Mp: 171.1 °C. ^{1}H NMR (300 MHz, DMSO-d_6) δ 7.969–7.938 (1H, m), 7.727 (1H, s), 7.723–7.583 (5H, m), 7.299–7.221 (2H, m), 7.122 (1H, s);^{13}C NMR (75 MHz, DMSO-d_6) δ159.581, 155.639, 140.014, 135.745, 132.261, 130.754, 128.713, 126.839, 126.660, 123.424, 122.886, 118.685, 117.022, 81.994 ppm; HRMS (ESI) *m*/*z* calcd for $C_{15}H_{10}N_2O_2$, 250.0742, found *m*/*z* 251.0737 (M+1).

Complex

The $Al(ClO_4)_3$ (0.1 mmol) was added to the ethanol solution containing **L** (0.1 mmol). The complex was obtained by stirring the mixture for 5 h. ESI-MS *m*/*z* calcd for $C_{34}H_{30}AlN_4O_6$, 617.2, found *m*/*z* 617.3. The $Al(ClO_4)_3$ (0.1 mmol) was added to the methanol solution containing **L** (0.1 mmol). The complex was obtained by stirring the mixture for 5 h. ESI-MS *m*/*z* calcd for $C_{32}H_{26}AlN_4O_6$, 589.2, found *m*/*z* 589.1.

Cell incubation and imaging

Human leukemia K562 cells were cultured in RPMI 1640 (Sigma, St. Louis, MO, USA) supplemented with 10% Fetal Bovine Serum (FBS, Rongye Biochem, Lanzhou) and penicillin (100 U ml^{-1})/streptomycin (100 mg L^{-1}). One day before imaging, cells were added into a sterile centrifuge tube, centrifuged to remove the top medium. Immediately before the experiments, cells were incubated with the probe **L** (50 μM) for 0.5 h in RPMI 1640 at 37 °C under 5% CO_2 and then washed with phosphate-buffered saline (PBS) three times. Next, cells were incubated with 25 μM $Al(ClO_4)_3$ for another 0.5 h, cells were rinsed with PBS three times again and then they were passed to 18 mm glass coverslips and imaged. The fluorescence imaging of intracelluar Al^{3+} was observed under an Olympus AX-80 laser scanning microscope with 10× and 40× oil-immersion objective lenses (excited with blue light). The HL K562 cells only incubated with 50 μM **L** for 0.5 h at 37 °C under 5% CO_2 were used as a control.

Acknowledgements

This study was supported by the NSFC (Grants Nos. 20771048, 20931003, 20621091). The Super Computing Center of Lanzhou University is thanked for the use of the facilities. The authors thank Dr Pamela Holt, Shandong University, for revising the manuscript.

References

1 (*a*) R. B. Martin, *Acc. Chem. Res.*, 1994, **27**, 204; (*b*) G. Fasman, *Coord. Chem. Rev.*, 1996, **149**, 125; (*c*) N. Fimreite, O. O. Hansen and H. C. Pettersen, *Bull. Environ. Contam. Toxicol.*, 1997, **58**, 1; (*d*) M. Venturini-Soriano and G. Berthon, *J. Inorg. Biochem.*, 2001, **85**, 143; (*e*) H. Bielarczyk, A. Jankowska, B. Madziar, A. Matecki, A. Michno and A. Szutowicz, *Neurochem. Int.*, 2003, **42**, 323.
2 M. Sargazi, N. B. Roberts and A. Shenkin, *J. Inorg. Biochem.*, 2001, **87**, 37.
3 M. I. Yousef, A. M. EI-Morsy and M. S. Hassan, *Toxicology*, 2005, **215**, 97.
4 (*a*) *Functional Synthetic Receptors*, ed. T. Schraderr and A. D. Hamilton, Wiley-VCH: Weinheim, Germany, 2005; (*b*) *Chemosensors of Ion and Molecule Recognition*, ed. J. P. Desvergne and A. W. Czarnik, Kluwer, Dordrecht, 1997; (*c*) *Fluorescent Chemosensors for Ion and Molecule Recognition*, ed. A. W. Czarnik, American Chemical Society, Washington, DC, 1992; (*d*) R. Martínez-Máñez and F. Sancenón, *Chem. Rev.*, 2003, **103**, 4419; (*e*) P. D. Beer and P. A. Gale, *Angew. Chem., Int. Ed.*, 2001, **40**, 486; (*f*) A. P. de Silva, H. Q. N. Gunaratne, T. Gunnlaugsson, A. J. M. Huxley, C. P. McCoy, J. T. Rademacher and T. E. Rice, *Chem. Rev.*, 1997, **97**, 1515.
5 (*a*) U. E. Spichiger-Keller, *Chemical Sensors and Biosensors for Medical and Biological Applications*, Wiley-VCH: Weinheim, Germany, 1998; (*b*) V. Amendola, L. Fabbrizzi, F. Forti, M. Licchelli, C. Mangano, P. Pallavicini, A. Poggi, D. Sacchi and A. Taglieti, *Coord. Chem. Rev.*, 2006, **250**, 273; (*c*) K. Rurack and U. Resch-Genger, *Chem. Soc. Rev.*, 2002, **31**, 116; (*d*) P. T. Srinivasan, T. Viraraghavan and K. S. Subramanian, *Water SA*, 1999, **25**, 47.
6 K. Soroka, R. S. Vithanage, D. A. Phillips, B. Walker and P. K. Dasgupta, *Anal. Chem.*, 1987, **59**, 629.
7 (*a*) N. Chattopadhyay, A. Mallick and S. Sengupta, *J. Photochem. Photobiol., A*, 2006, **177**, 55; (*b*) Y. G. Zhao, Z. H. Lin, H. P. Liao, C. Y. Duan and Q. J. Meng, *Inorg. Chem. Commun.*, 2006, **9**, 966.
8 (*a*) L. Salmon, P. Thuéry, E. Rivière and M. Ephritikhine, *Inorg. Chem.*, 2006, **45**, 83; (*b*) D. M. Epstein, S. Choudhary, M. R. Churchill, K. M. Keil, A. V. Eliseev and J. R. Morrow, *Inorg. Chem.*, 2001, **40**, 1591.
9 V. C. Da Silveira, J. S. Luz, C. C. Oliveira, I. Graziani, M. R. Ciriolo and A. M. Ferreira, *J. Inorg. Biochem.*, 2008, **102**, 1090.
10 (*a*) S. Padhye and G. B. Kauffman, *Coord. Chem. Rev.*, 1985, **63**, 127; (*b*) Y. Li and Z. Y. Yang, *Inorg. Chim. Acta*, 2009, **362**, 4823.
11 S. Kasselouri, A. Garoufis, A. Katehanakis, G. Kalkanis, S. P. Perlepes and N. Hadjiliadis, *Inorg. Chim. Acta*, 1993, **207**, 255.
12 E. Cielen, A. Stobiecka, A. Tahri, G. J. Hoornaert, F. C. De Schryver, J. Gallay, M. Vincent and N. Boens, *J. Chem. Soc., Perkin Trans.*, 2002, **2**, 1197.

13 W. C. Vosburgh and G. R. Cooper, *J. Am. Chem. Soc.*, 1941, **63**, 437.
14 (*a*) M. Cametti, A. Dalla Cort, M. Colapietro, G. Portalone, L. Russo and K. Rissanen, *Inorg. Chem.*, 2007, **46**, 9057; (*b*) A. Ben Othman, J. W. Lee, Y. D. Huh, R. Abidi, J. S. Kim and J. Vicens, *Tetrahedron*, 2007, **63**, 10793.
15 (*a*) G. M. Sheldrick, *SHELXL-97, Program for the Solution of Crystal Structures*, University of Göttingen: Göttingen, Germany, 1997; (*b*) G. M. Sheldrick, *SHELXL-97, Program for the Refinement of Crystal Structures*, University of Göttingen: Göttingen, Germany, 1997.
16 A. L. Spek, *PLATON*, Utrecht University, Utrecht, The Netherlands, 1998.